Alloying Mechanisms for Epitaxial Nanocrystals

M. S. Leite,[1,2] G. Medeiros-Ribeiro,[1,3,*] T. I. Kamins,[3] and R. Stanley Williams[3]

[1]*Laboratório Nacional de Luz Síncrotron, Caixa Postal 6192, CEP 13083-970, Campinas, SP, Brazil*

[2] *Instituto de Física Gleb Wataghin, Universidade Estadual de Campinas, CP 6165, 13083-970, Campinas, SP, Brazil*

[3]*Hewlett-Packard Laboratories, 1501 Page Mill Road, 94304 Palo Alto, California, USA*

(Received 26 October 2006; published 18 April 2007)

The different mechanisms involved in the alloying of epitaxial nanocrystals are reported in this Letter. Intermixing during growth, surface diffusion, and intraisland diffusion were investigated by varying the growth conditions and annealing environments during chemical vapor deposition. The relative importance of each mechanism was evaluated in determining a particular composition profile for dome-shaped Ge:Si (001) islands. For samples grown at a faster rate, intermixing during growth was reduced. Si surface diffusion dominates during H_2 annealing, whereas Ge surface diffusion and intraisland diffusion prevail during annealing in a PH_3 environment.

DOI: 10.1103/PhysRevLett.98.165901 PACS numbers: 66.30.Pa, 68.35.Dv, 68.35.Fx, 81.10.Aj

In coherently strained epitaxial islands, the most important factor that determines island size and stability is composition. Composition variations inside these nanocrystals will substantially influence their structural properties and, as a consequence, the associated electronic properties [1]. The understanding of this issue has been addressed theoretically by Monte Carlo (MC) simulations [2,3], but the pathways that lead to particular composition configurations have not been fully explored. The composition profile of SiGe islands has only recently been measured [4–6], and its origin depends on kinetic and thermodynamic contributions, which sometimes are difficult to separate.

Alloying in coherently strained nanocrystals needs to be investigated in more detail to understand island formation and evolution. The primary mechanisms that modulate the composition profile of self-assembled islands are (a) exchange reactions between Si and Ge during island growth, defined by the attachment and detachment of atoms between the crystal and 2D adatom gas, (b) surface diffusion of both Si and Ge adatoms, and (c) diffusion of Ge and Si atoms within the islands (intraisland diffusion), excluding the surface adatoms. In order to comprehend the composition profiles, it is imperative to vary the kinetic and thermodynamic components individually in experiments to elucidate the mechanisms that lead to intermixing for a particular growth condition. Adjusting the growth and annealing parameters allow us to privilege one mechanism at a time, but not rigorously suppress the other two.

Changing the deposition rate in molecular beam epitaxy (MBE) grown islands allowed the control of the Ge content via atom exchange (a) and surface diffusion (b) [7]. In a careful and detailed study [8], some of the pathways for Si and Ge intermixing have been investigated in islands grown at different temperatures with subsequent annealing steps in UHV. The main result for the reported experimental conditions was that surface diffusion of Si and Ge was the dominant mechanism determining the island composition profile [8]. It is known, however, that growth and annealing in different ambient conditions (i.e., UHV, as opposed to H_2 or PH_3 environments) selectively changes the surface mobility of adatoms [9,10]. As a result, alloying in the presence of gases can proceed privileging selected mechanisms during chemical vapor deposition (CVD) growth.

Bulk diffusion requires the formation of vacancies and/or interstitials [11]. For buried 2D SiGe layers, diffusion of Ge was found to increase with the Ge content and compressive stress [12]. Although the amount of diffusion inferred from these results extrapolated to 600 °C is negligible for unstrained material, the activation energies depend strongly on strain. For the case of submonolayer coverages, even at temperatures around 500 °C, Ge diffusion and intermixing into Si surfaces has been theoretically predicted and was observed by high resolution Rutherford backscattering (RBS) before the first monolayer of material was completely deposited [13,14]. In self-assembled islands, a significant amount of strain is present and the fact that high index facets and edges (and hence defects) make up the surface provides a larger number of pathways for intermixing compared to a 2D film. However, experimental results of intraisland diffusion (c) are inconclusive [8].

The goal of this work is to evaluate the relative importance of each mechanism by comparing samples grown by CVD and annealed under different conditions. For instance, comparing samples grown at different rates affects all mechanisms, but more effectively (a) and (b). Annealing in a H_2 environment decreases surface mobility of both Ge and Si compared to annealing in UHV [9], yet does not completely stop the surface diffusion of either species. Thus it allows both mechanisms (b) and (c) to be investigated. Annealing in a PH_3 environment substantially reduces Si surface diffusion, yet has little effect on Ge surface diffusion. This different behavior occurs because the P-Si bond is stable (bond enthalpy equal to 364 ± 7 kJ/mol), whereas the P-Ge bond is unstable [15]. In

 © 2007 The American Physical Society

this case, mechanism (c) dominates for both Ge and Si species, and mechanism (b) persists for Ge adatoms.

Four samples with nominally the same Ge deposition thickness of 12 eq-ML (1eq-ML $= 6.3 \times 10^{14}$ atoms/cm^2) were grown at 600 °C in a H_2 ambient in a commercial CVD reactor on 150 mm diameter Si (001) wafers. The conditions were chosen to produce dome-shaped islands. The reproducibility of film thickness from run to run as determined by RBS analysis was better than 5%. The first two samples were grown at $P(GeH_4) = 5 \times 10^{-4}$ Torr [as-deposited fast (F), 6 eq-ML/min] and $P(GeH_4) = 2.5 \times 10^{-4}$ Torr [as-deposited slow (S), 3 eq-ML/min] in a 10 Torr ambient composed mainly of H_2 and immediately cooled to room temperature. The other two samples were grown at the same rate as sample S (reference sample); however, after deposition of the Ge film they were subsequently annealed *in situ* for 10 min at the growth temperature (600 °C) in PH_3/H_2 with up to 1.4×10^{-5} Torr added PH_3 (annealed P) or H_2 (annealed H) environments. The samples were characterized initially by reciprocal-space mapping (RSM) using a conventional Cu$K\alpha$ x-ray tube using the (224) and (004) reflections in order to extract the average Ge content [16]. Selective chemical etching in 25%NH_4OH:31%H_2O_2 room temperature solution for varying times was used to study the composition profiles in more detail. This etchant is known to be more sensitive to the Ge concentration variations than the RSM measurements, and to slowly remove Ge-rich SiGe alloys with exponentially varying Ge selectivity [17,18], allowing a detailed study of the remaining material. Although the absolute composition obtained from this technique is not known with a high precision as anomalous x-ray diffraction [4,19] or electron-energy-loss spectroscopy (EELS) in a scanning transmission electron microscope (STEM) [7,20], the relative comparisons between samples are far more sensitive than either method. For this work our conclusions rely primarily on the comparative analysis rather than on the knowledge of the absolute content. Local and statistical analyses were performed for the as-grown and etched samples with atomic force microscopy (AFM) over ensembles of about 400 islands per etching condition.

Table I shows a summary of the growth parameters used and the average Ge composition obtained through the RSM experiments. Samples as-deposited F and S and annealed P were found to have the same average Ge content within the experimental uncertainties. However, a lower Ge content was found for sample annealed H, accompanied by a broader diffraction peak corresponding to a wider distribution of compositions within the island ensemble (not shown). These results suggest that Si surface diffusion plays an important role in the final composition profile for sample H, whereas for the other samples that mechanism is minimal. This also confirms the low surface diffusivity of Si in a PH_3 environment. The last column displays the total integrated amount of material in the islands, which is consistent with the total amount of Ge deposited of 12.0 ± 0.5 ML and the 3.5 ML thick wetting layer.

Figure 1 shows the evolution of all samples before and after etching for 30 min and 60 min. The top images correspond to 250 nm × 250 nm AFM scans, and the bottom graphs correspond to line profiles taken on statistically representative islands selected from height histograms. The different profiles indicate different degrees of alloying. After 4 hours of etching, the entire island material was removed for all cases, leaving a visible moat around the region where the islands were previously located (not shown).

Comparing the AFM images and the line scans before etching, we found that the domes of sample annealed H are slightly larger in diameter; their height is the same as for the dome islands of sample as-deposited S. By comparing samples S and annealed P, three main observations can be made for sample P: (i) the domes are slightly taller, (ii) the island's total integrated volume is significantly larger, and (iii) there are no pyramids. From these observations we can conclude that in addition to Ge surface diffusion from pyramids to domes, material from the substrate is effectively being incorporated into the islands causing their growth (comparing samples S and P this amounts to roughly 4 ± 3 ML). This has been observed recently also by STEM-EELS experiments in samples annealed at 650 °C [20], producing a nonabrupt yet uniform interface.

All but sample annealed H consisted of a symmetric Ge-rich outer shell as shown previously by grazing incidence anomalous x-ray diffraction (GIXD) experiments [4]. For sample H, an irregular composition profile is revealed by the selective etching, as seen in Fig. 1. This has been observed previously in CVD grown samples [21], and more recently for MBE grown material [17], and both are consistent with a significant amount of Si surface diffusion and concomitant intermixing. This asymmetric alloying profile is in accord with the GIXD results of wider

TABLE I. Growth parameters and average Ge content in each sample obtained through reciprocal-space mapping using a conventional X-ray tube. The integrated thickness corresponds to the total island volume material integrated per area, not including the wetting layer. The samples were grown by CVD, at 600 °C.

Sample	Growth rate (ML/min)	Annealing	⟨Ge%⟩	Integrated thickness (ML)
As-deposited F	6	No	64 ± 5	6.5 ± 1.5
As-deposited S	3	No	63 ± 5	7.0 ± 1.5
Annealed P	3	10′ PH_3	64 ± 5	11 ± 1.5
Annealed H	3	10′ H_2	53 ± 5	6.5 ± 1.5

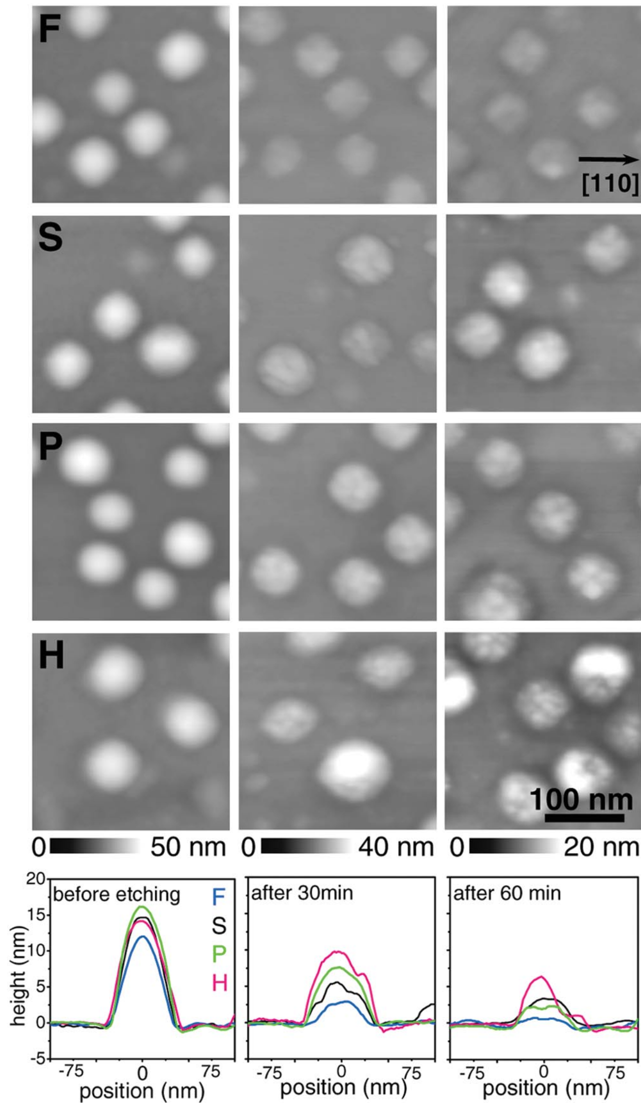

FIG. 1 (color). AFM images and line scans (bottom) of representative dome islands of all samples as grown, after 30 min and after 60 min of etching with 25%NH_4OH:31%H_2O_2.

composition range within the islands. For sample H, Si and Ge surface diffusion [mechanism (b)] and possibly intraisland diffusion [mechanism (c)] act together producing the observed morphology.

For all etching times, sample as-deposited F exhibited a larger fraction of removed material, indicating that intermixing during growth [mechanism (a)] as well as the other mechanisms are reduced by the shorter growth time. A recent report [7] on MBE grown material portrayed similar results.

After 30 min of etching, the domes in sample as-deposited S have a top that is richer in Ge compared to sample annealed P. After 60 min of etching, one finds that more material has been removed from sample P in contrast to sample as-deposited S and annealed H, associated with a Ge-rich region in sample P. These facts demonstrate that Ge and Si redistribute inside the island during annealing in PH_3, with Ge diffusing down toward the island base, and Si diffusing up toward the island apex. Comparing the inferred profile to results of MC simulations, which allow for intraisland diffusion [2,3], experiment and simulation both show a SiGe core and a Ge-rich shell.

Summarizing the above results, height statistics for samples as grown and after etching for 30 and 60 min are shown in Fig. 2. For samples F, S, H, and P, the island heights are 12.4 ± 2.1, 14.3 ± 2.3, 14.1 ± 2.8, and 16.1 ± 2.3 nm, respectively. The error bars correspond to the standard deviation σ of the island height distributions. The line scans (bottom of Fig. 1), together with the height statistics, show that for the top 7–8 nm samples annealed P and H are richer in Si when compared to samples as-deposited S and F. This situation is different for the bottom 5 nm, where samples annealed P and as-deposited F exhibit a Ge-rich base. From the evolution of σ with etching, one finds that sample annealed H has a consistently broader dome height distribution than the others, indicating a wider composition range within the island ensemble.

The sequence of line scans and height statistics shows that the etching rate is not uniform, confirming that the Ge concentration in the island is not constant in the growth direction. In Fig. 3, the total integrated volume is shown as a function of the etching time. The slope of the curve is associated with the average Ge content in the film, increasing from sample H to S, to P, and finally F. Comparing samples S and F shows that faster Ge deposition results in an increase of the Ge amount in the islands, corresponding to less intermixing during growth [7]. While sample annealed H is richer in Si compared to the reference sample (S), annealing in PH_3 enriches the Ge content compared to sample S. This demonstrates that surface diffusion processes can be selectively controlled depending on the proper choice of the annealing environment.

To understand the intraisland diffusion contribution to the alloy formation, a more detailed analysis was carried out for sample annealed P, where this particular process could be more clearly isolated. The composition profile was studied by sequentially etching and taking line scans along the [110] direction on the same representative island. Figure 4(a) shows line scans for an island before etching and after etching to $h(x, y) < 5$ nm. At this particular

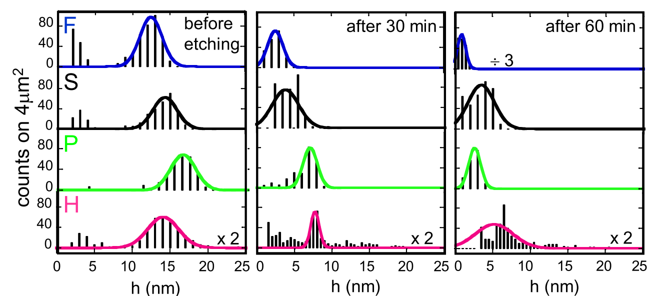

FIG. 2 (color online). Height statistics as a function of etching time.

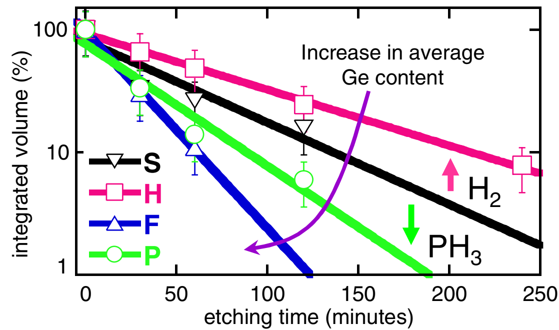

FIG. 3 (color online). Total integrated volume (%) as a function of the etching time (minutes) for all samples. The slope of the curve is associated with the average Ge content in the film, with material being removed faster for Ge-rich SiGe regions.

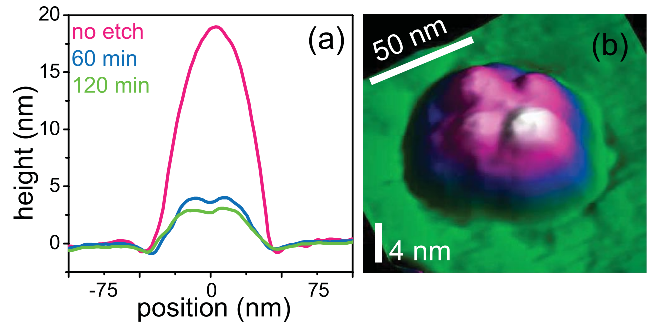

FIG. 4 (color). Sample annealed P: (a) Line scans on the same island as grown and after two etching steps. (b) 3D AFM image of one representative dome after 60 min of etching, showing the rosette final morphology.

height, sample P exhibited a Ge content higher than all samples except sample as-deposited F, indicating Ge diffusion toward the island base (intraisland diffusion). The region after etching shows a smaller diameter and height than prior to etching, consistent with a Ge-rich shell. It also shows a small dip at the center, corresponding to a Ge-rich apex, similar to low temperature MC simulations [3]. In Fig. 4(b), a 3D AFM image exhibits a statistically significant rosette pattern, produced by atom redistribution within the island. This observation is associated with strain-assisted intraisland diffusion. Similar morphology has been previously reported, also in a post-growth annealing experiment [5], and was attributed to enhanced surface diffusion, which occurred at the island edges. However, in the present work, alloying takes place inside the island, and the edges remain Ge rich, as can be seen in the line profiles of Fig. 4(a); thus no Si could have come from the surface. The driving forces in both experiments are basically the same—minimization of elastic energy and maximization of entropy [3,22].

The Si-rich regions occur along the [110] directions. Since the facet angle of the bounding {311} facets is less steep than the {15 3 23} facets (25° and 32°, respectively) a smaller strain relaxation can take place in the [110] direction. Therefore, Ge moves towards the soft [010] directions and Si moves to the [110] direction, thus producing the rosette structure. At the center of the rosette, one also finds a Ge-rich region, presumably reflecting more efficient relaxation at that site. The enhanced intraisland diffusion occurs only very close to the substrate (about 4 nm from the surface of an otherwise pristine island 16 nm high), where the strain is large [23].

In summary, a systematic study focused on the intermixing mechanisms in Ge:Si(001) islands was carried out. Samples were grown and annealed in different environments allowing different diffusion processes to dominate. Selective etching and the RSM experiments permitted a semiquantitative picture of the Ge content profile inside the dome islands. Increasing the growth rate decreased the degree of Si-Ge intermixing. Intraisland diffusion occurred during annealing in different environments, but surface diffusion could be varied selectively by controlling the ambient gas. When Si surface diffusion was minimized, atomic rearrangement took place within the islands via intraisland diffusion, leading to a fourfold symmetric rosette structure.

The authors acknowledge A. Rastelli and G. Katsaros for fruitful discussion, and N. J. Quitoriano for his invaluable help in RSM. M. S. L. and G. M. R. thank FAPESP Contract No. 03/09374-9, CNPq, and HPBrazil for financial support.

*Corresponding author.
Email address: gmedeiros@lnls.br

[1] J. Tersoff, Phys. Rev. Lett. **81**, 3183 (1998).
[2] G. Hadjisavvas *et al.*, Phys. Rev. B **72**, 075334 (2005).
[3] C. Lang *et al.*, Phys. Rev. B **72**, 155328 (2005).
[4] A. Malachias *et al.*, Phys. Rev. Lett. **91**, 176101 (2003).
[5] U. Denker *et al.*, Phys. Rev. Lett. **90**, 196102 (2003).
[6] Margaret Floyd *et al.*, Appl. Phys. Lett. **82**, 1473 (2003).
[7] E. P. McDaniel *et al.*, Appl. Phys. Lett. **87**, 223101 (2005).
[8] G. Katsaros *et al.*, Phys. Rev. B **72**, 195320 (2005).
[9] T. I. Kamins *et al.*, J. Appl. Phys. **94**, 4215 (2003).
[10] T. I. Kamins *et al.*, J. Appl. Phys. **95**, 1562 (2004).
[11] P. Fahey *et al.*, Appl. Phys. Lett. **54**, 843 (1989).
[12] N. R. Zangenberg *et al.*, Phys. Rev. Lett. **87**, 125901 (2001).
[13] Blas P. Uberuaga *et al.*, Phys. Rev. Lett. **84**, 2441 (2000).
[14] Kaoru Nakajima *et al.*, Phys. Rev. Lett. **83**, 1802 (1999).
[15] *CRC Handbook of Chemistry and Physics*, edited by D. R. Lide (CRC Press, Boca Raton, 2000), 81st ed.
[16] P. van der Sluis, J. Phys. D **26**, A188 (1993).
[17] U. Denker *et al.*, Phys. Rev. Lett. **94**, 216103 (2005).
[18] G. Katsaros *et al.*, Surf. Sci. **600**, 2608 (2006).
[19] T. U. Schülli *et al.*, Phys. Rev. Lett. **90**, 066105 (2003).
[20] R. R. Vanfleet *et al.*, Appl. Phys. A **86**, 1 (2007).
[21] T. I. Kamins *et al.*, Appl. Phys. A **67**, 727 (1998).
[22] G. Medeiros-Ribeiro *et al.*, Nano Lett. **7**, 223 (2007).
[23] R. Magalhaes-Paniago *et al.*, Phys. Rev. B **66**, 245312 (2002).